nature climate change

Brief Communication

https://doi.org/10.1038/s41558-024-02088-x

Accelerated warming in the North Pacific since 2013

Received: 25 September 2023

Accepted: 9 July 2024

Published online: 23 July 2024

Check for updates

Zeng-Zhen Hu [1] ✉, Michael J. McPhaden [2], Boyin Huang [3], Jieshun Zhu [1] & Yunyun Liu [4]

Sea surface temperature increase in the global ocean exhibits marked spatial and temporal variations, with warming in the North Pacific significantly higher than in other basins since 2013. This accelerated warming is related to a shoaling of ocean surface mixed-layer depth and is partially dampened by an increase in anomalous net surface heat flux from the ocean. Among heat-flux components, latent heat flux is dominant.

The increase in global ocean temperature during the past few decades has been well documented[1–3]. However, the warming trends vary both spatially and temporally. For example, in the tropical Pacific, where El Niño/Southern Oscillation events occur every 3–7 years, there has been an appreciable warming trend in the west and minor cooling tendencies in the east[4–6]. The strengthened zonal mean sea surface temperature (SST) contrast across the tropical Pacific driven by enhanced trade winds was a crucial driver for the triple-dip La Niña in 2020–2023 (ref. 6). Recently, it has been noted that, compared with SST trends in the tropical Pacific (30° S–30° N), the tropical Indian Ocean (30° S–30° N), the North Atlantic (30° N–60° N), the tropical Atlantic (30° S–30° N) and the Southern Ocean (30° S–60° S), the SST warming trend in the North Pacific (30° N–60° N) was largest during 2000–2022 (ref. 3). The accelerated warming in the North Pacific was manifested in part by marine heatwaves over the past decade, notably the 'Blob' in 2014–2016 (refs. 7,8) and a later pronounced marine heatwave in 2019 (ref. 9).

Referring to the mean in 1981–2010 as the baseline for comparison, the SST anomaly (SSTA) averaged in 2013–2023 was the highest in the North Pacific compared with other basins (Fig. 1a,b). Temporally, during 2000–2012 (Fig. 1c,d), the SSTA changes averaged for the global ocean (60° S–60° N; curve) and North Pacific (20° N–60° N, 120° E–110° W; shading) were comparable and relatively small associated with the hiatus in global warming[10]. However, since 2013, positive anomalies in the North Pacific have exceeded those for the global ocean with the differences in SSTA changes indicating a faster warming in the North Pacific compared with the global ocean. The SSTA difference pattern and temporal evolution based on version 5 of the Extended Reconstructed SST (ERSSTv.5; Fig. 1a,c) and the UK Met Office Hadley Centre's monthly mean global sea ice and SST data (HadISST; Fig. 1b,d) are similar to those based on the latest version of Optimum Interpolation SSTs (OIv.2.1) and the Operational Sea Surface Temperature and Ice Analysis (OSTIA) SST (see Methods), indicating the robustness of the SSTA spatial and temporal variations.

Zonally averaged SSTA shows that the remarkable warming that emerged in the North Pacific around 2013 was stronger than that observed in the South Pacific (Fig. 1e,f). Maximum warming in the North Pacific varied with latitude during 2013–2023, with positive anomalies present mainly in the low (20° N–30° N) and high (50° N–60° N) latitudes during 2014–2017 and in the middle latitudes (30° N–50° N) since 2018. The accelerated warming in the North Pacific may not be simply related to well-known modes of natural climate variability such as the Pacific Decadal Oscillation (PDO)[11]. The PDO spatial pattern flips sign between the eastern and western North Pacific in contrast to observed basin-scale warming between 20° N and 60° N during January 2013–December 2023. The PDO has tended towards negative values over the past decade, which might account for some of the observed warming in the western North Pacific, but not in the eastern North Pacific, where the largest warming was observed (Fig. 1a,b). Indeed, relative to a baseline of January 1981–December 2010, the pattern correlation between the PDO SSTA and observed SSTA over January 2013–December 2023 in the North Pacific is only 0.30. This result suggests that PDO cannot be the major factor accounting for the domain-averaged warming in the North Pacific for this period.

Associated with the accelerated SST warming in the North Pacific, the depth of the ocean mixed layer (OML; Fig. 2a) shoaled most notably between 40° N and 60° N since 2013. A shallower OML means that the OML has a lower heat capacity so that the same downward heat flux can lead to a larger near-surface warming. For example, it has been suggested that multi-decadal shoaling of OML was a contributor to the 2019 Northwest Pacific marine heatwave and that anthropogenic OML shoaling would amplify marine heatwaves in a warmer climate[7]. It was further argued that global warming may shoal the OML due

[1]NOAA/NCEP Climate Prediction Center, College Park, MD, USA. [2]NOAA/Pacific Marine Environment Laboratory, Seattle, WA, USA. [3]NOAA National Centers for Environmental Information, Asheville, NC, USA. [4]CMA Climate Study Key Laboratory, National Climate Center, China Meteorological Administration, Beijing, China. ✉e-mail: Zeng-Zhen.Hu@NOAA.GOV

https://doi.org/10.1038/s41558-024-02088-x

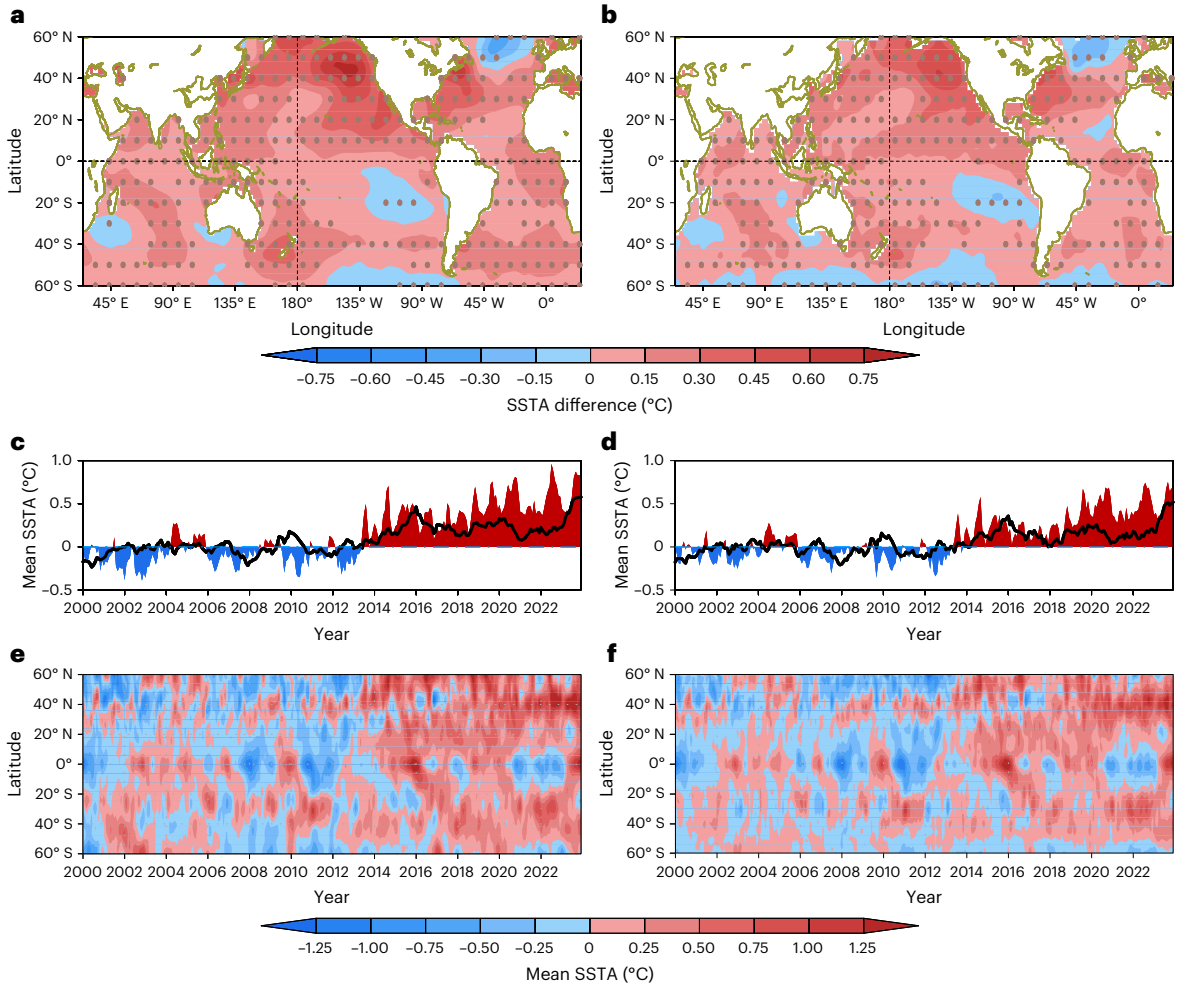

Fig. 1 | SSTA in the global ocean and the North Pacific. a,**b**, Mean SSTA differences between January 2013–December 2023 and January 1981–December 2010 from ERSSTv.5 (**a**) and HadISST (**b**). **c**,**d**, Monthly mean SSTA averaged in the global ocean (60° S–60° N; curve) and the North Pacific (20° N–60° N, 120° E–110° W; shading) for January 2000–December 2023 from ERSSTv.5 (**c**) and HadISST (**d**). **e**,**f**, Zonally averaged (120° E–110° W) monthly mean SSTA for January 2000–December 2023 from ERSSTv.5 (**e**) and HadISST (**f**).

mainly to increasing upper-ocean stability[12]. Thus, the OML shoaling in the North Pacific, which is potentially driven by global warming, appears to be a crucial contributor to the warming in the North Pacific since 2013 (ref. 3).

Anomalous surface heat fluxes can also affect SST. On average, there has been an anomalous net heat flux from the ocean to the atmosphere during 2013–2023 (mainly in the mid-latitudes, 20° N–40°:N; Fig. 2b,c), to dampen the warming in the North Pacific. The increased heat loss from the ocean to the atmosphere in the North Pacific has been noted for net heat flux during 1988–2005 (ref. 13) and latent heat flux during 1988–2008 (ref. 14). The increase may be linked to multiple factors, including an increase in wind speed, an increase in sea surface saturated air humidity and a decrease in near-surface air humidity[13,14]. However, we also note a large increase of net downward heat flux (from atmosphere to ocean) over the shallowed mixed layer in a large part of the North Pacific, north of 40° N and the Kuroshio Extension (Fig. 2a,b), which contributes to the warming.

Quantitatively, for the average observed SSTA warming of 0.59 °C over 2013–2023 compared with the baseline in 1981–2010 in the North Pacific (20° N–60° N; 120° E–110° W; Fig. 2d), about 119% (equivalent to 0.70 °C) was related to OML shoaling. This warming was partially offset by an increased anomalous net heat flux out of the ocean equivalent to −0.14 °C, or 24% of the total warming. Among the surface heat-flux components, latent heat flux by itself would have produced a cooling of −0.14 °C over the past decade (black narrow bar in Fig. 2d). Thus, latent heat flux determined the sign, magnitude and spatial structure the of anomalous oceanic heat loss over this period (Fig. 2b,c), consistent with previous analyses[14]. The nonlinear term based on the covariance of OML and surface heat flux (third term on the right side of equation (3)) represents a negligible cooling effect of −0.07 °C, equivalent to 1% of the overall SSTA warming. Adding for all the terms (0.56 °C) accounts for 95% of the total warming (0.59 °C).

How much of this accelerated warming results from processes internal to the North Pacific compared with remote forcing from higher or lower latitudes, or from other ocean basins, is an open question. Likewise, the extent to which SST warming, upper-ocean stabilization and OML shoaling may reinforce one another to further accelerate warming in the North Pacific is an important question. Our analysis of the surface heat balance has shown that accelerated warming in the North Pacific since 2013 has been favoured by shoaling of the OML and dampened by increased latent heat flux from the ocean surface. However, our heat budget analysis addresses only the effects of heat storage in the OML as it influences SST warming. We have not closed the heat balance (Fig. 2d), and other terms that we did not explicitly compute (for example, lateral advection, eddy transports and/or vertical entrainment) must also be important. Assessing these mechanisms is a necessary next step but one which is beyond the scope of this short note.

https://doi.org/10.1038/s41558-024-02088-x

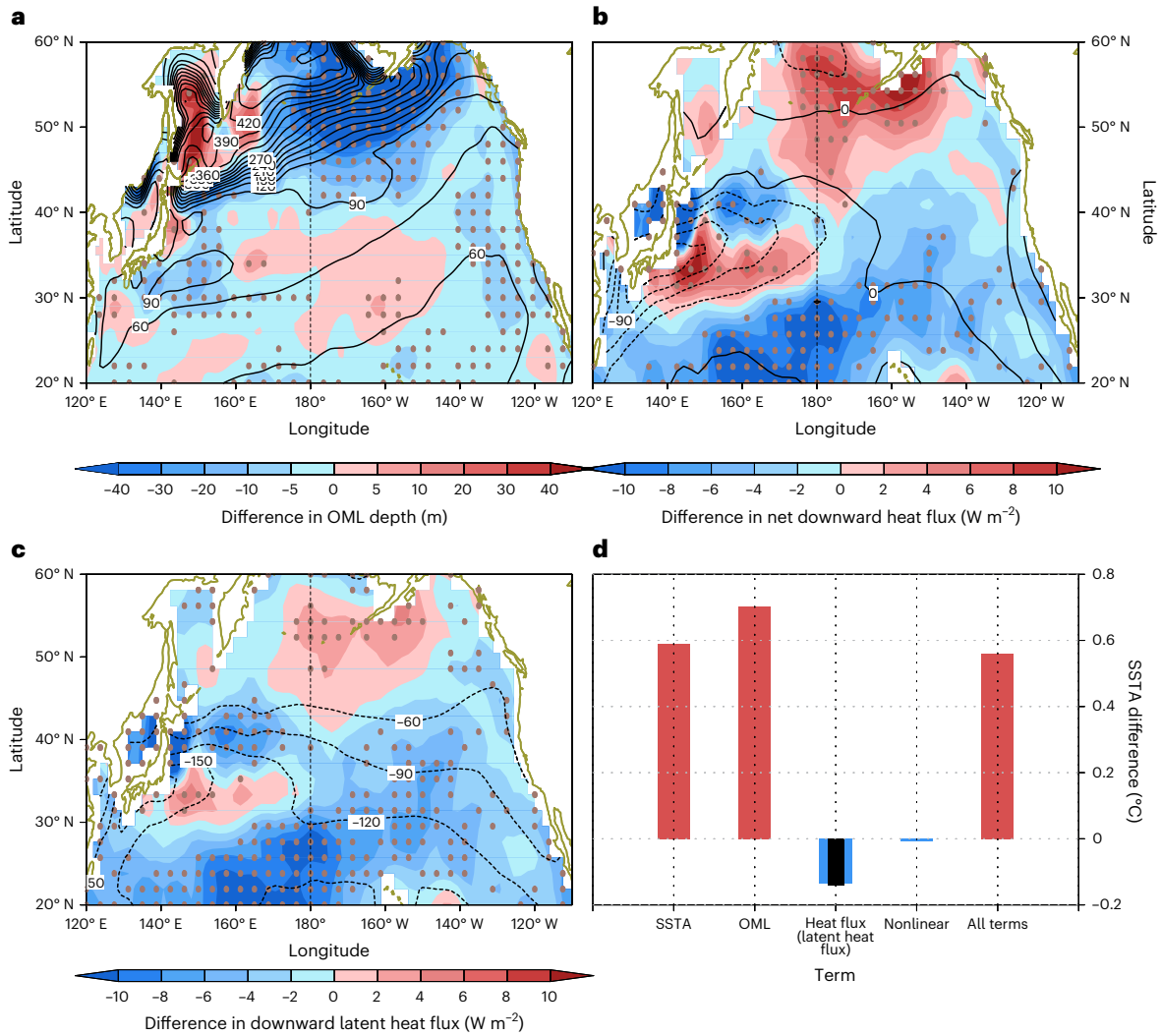

Fig. 2 | Causes of the warming in the North Pacific. a–**c**, Mean (contours) in January 1981–December 2010 and differences (shading) of OML depth (m) (**a**), net downward heat flux (W m^{-2}) (**b**) and net downward latent heat flux at the ocean surface (W m^{-2}) (**c**) between January 2013–December 2023 and January 1981–December 2010. Dots in **a**–**c** denote significant differences at the 5% level using a *t* test. **d**, SSTA differences of each term based on equation (3) compared with the observed SSTA differences averaged in 20° N–60° N, 120° E–110° W. The black narrow bar in **d** represents the corresponding latent heat-flux component. Positive (negative) anomalies in **a** mean deeper (shallower) OML; positive anomalies in **b**,**c** represent increased heat flux from the atmosphere to the ocean (a warming effect) while negative anomalies represent increased heat flux from the ocean to the atmosphere (a cooling effect).

Online content

Any methods, additional references, Nature Portfolio reporting summaries, source data, extended data, supplementary information, acknowledgements, peer review information; details of author contributions and competing interests; and statements of data and code availability are available at https://doi.org/10.1038/s41558-024-02088-x.

References

1. IPCC *Climate Change: The Physical Science Basis* (eds Masson-Delmotte, V. et al.) (Cambridge Univ. Press, 2021).
2. Cheng, L. et al. *Adv. Atmos. Sci.* https://doi.org/10.1007/s00376-023-2385-2 (2023).
3. Yin, X. et al. *Bull. Amer. Meteorol. Soc.* **104**, S153–S156 (2023).
4. Hu, Z.-Z. et al. *J. Clim.* **26**, 2601–2613 (2013).
5. Lee, S. et al. *npj Clim. Atmos. Sci.* **5**, 82 (2022).
6. Li, X., Hu, Z.-Z., McPhaden, M. J., Zhu, C. & Liu, Y. *J. Geophys. Res.* **128**, e2023JD038843 (2023).
7. Bond, N. A., Cronin, M. F., Freeland, H. & Mantua, N. *Geophys. Res. Lett.* **42**, 3414–3420 (2015).
8. Hu, Z.-Z., Kumar, A., Jha, B., Zhu, J. & Huang, B. *J. Clim.* **30**, 689–702 (2017).
9. Amaya, D. J. et al. *Bull. Am. Meteorol. Soc.* **102**, S59–S66 (2021).
10. Fyfe, J. et al. *Nat. Clim. Change* **6**, 224–228 (2016).
11. Mantua, N. J., Hare, S. R., Zhang, Y., Wallace, J. M. & Francis, R. C. *Bull. Am. Meteorol. Soc.* **78**, 1069–1079 (1997).
12. Shi, H. et al. *Sci. Adv.* **8**, eabm3468 (2022).
13. Iwasaki, S. & Kubota, M. *Geophys. Res. Lett.* **38**, L10604 (2011).
14. Gao, S., Chiu, L. S. & Shie, C.-L. *Geophys. Res. Lett.* **40**, 380–385 (2013).

Methods

Monthly mean global SSTs on a 2 × 2 grid are from ERSSTv.5 since January 1854 (ref. 15), which are derived from the SST of the International Comprehensive Ocean–Atmosphere Dataset Release 3.0 (ICOADS) and Argo floats above 5 m, and HadISST2 ice concentration. The improvements in ERSSTv.5 include (1) reducing spatial filtering in training the reconstruction functions empirical orthogonal teleconnections (EOTs), (2) removing high-latitude dampening in EOTs and (3) adding ten more EOTs in the Arctic.

To verify the robustness of the results, we also used the HadISST[16], the monthly mean SSTs from OIv.2.1 (ref. 17) and OSTIA[18]. The HadISST is on a 1° latitude–longitude grid from 1870 to present. The SST data are taken from the Met Office Marine Data Bank (mainly ship tracks) and ICOADS through 1981 and a blend of in situ and adjusted satellite-derived SSTs for 1982 onwards. The 'bucket correction' was applied to SSTs for 1871–1941 to correct biases caused by instrument changes. The OIv.2.1 monthly mean SSTs are available since September 1981; they are computed from the latest version of daily OIv.2.1 SSTs. OIv.2.1 incorporates observations from different platforms (satellites, ships, buoys and Argo floats) into a regular global grid. Satellite and ship observations are referenced to buoys to compensate for platform differences and sensor biases. The OSTIA monthly mean SSTs are available since January 1985; they are computed from the daily SST that is determined by satellite data from both infrared and microwave radiometers together with in situ observations.

Monthly mean heat fluxes are derived from ERA5 (the fifth-generation European Centre for Medium-Range Weather Forecasts atmospheric reanalysis)[19], and monthly mean depth of the OML is from the Global Ocean Data Assimilation System[20] for the period from January 1979 to December 2023. The anomalies are relative to the climatologies of 1991–2020.

For the heat balance in OML:

$$\frac{\partial T}{\partial t} = \frac{Q}{\rho C_p h} + \text{Advection} + \text{Mixing} \quad (1)$$

where t is time, T is SST, Q is the downward net heat flux at the ocean surface, ρ is water density (=1,020 kg m^{-3}), C_p is heat capacity (=4,187 J kg^{-1} °C^{-1}) and h is the depth of the OML. Let

$$T = T_0 + T'$$

$$Q = Q_0 + Q'$$

$$H = h_0 + h'$$

where the subscript zero denotes mean values, and the prime represents the change from the mean. By ignoring the advection and mixing changes, the heat balance for the mean state is

$$\frac{\partial T_0}{\partial t} = \frac{Q_0}{\rho C_p h_0} \quad (2)$$

with $(h')^2 \ll (h_0)^2$, then,

$$\frac{\partial T'}{\partial t} = \frac{Q_0 + Q'}{\rho C_p (h_0 + h')} - \frac{Q_0}{\rho C_p h_0} \approx \frac{Q'}{\rho C_p h_0} - \frac{Q_0 h'}{\rho C_p h_0^2} - \frac{Q' h'}{\rho C_p h_0^2} \quad (3)$$

In this analysis, Q_0 and h_0 are represented by their monthly climatological values in 1991–2020. The differences are defined as between the means in January 2013–December 2023 and in January 1981–December 2010. The significance of the differences is tested at the 5% level using a t test.

Data availability

The ERSSTv.5 (ref. 15), HadISST SST[16], OIv.2.1 SST[17], OSTIA SST[18], ERA5 (ref. 19) and GODAS[20] reanalyses can be downloaded from https://psl.noaa.gov/data/gridded/data.noaa.ersst.v5.html, http://hadobs.metoffice.com/hadisst/data/download.html, https://www.ncei.noaa.gov/products/optimum-interpolation-sst, https://ghrsst-pp.metoffice.gov.uk/ostia-website/index.html, https://climatedataguide.ucar.edu/climate-data/era5-atmospheric-reanalysis and https://www.esrl.noaa.gov/psd/data/gridded/data.godas.html, respectively.

Code availability

The GrADS (http://cola.gmu.edu/grads/) was used to perform the analysis and generate all the plots in this paper.

References

15. Huang, B. et al. *J. Clim.* **30**, 8179–8205 (2017).
16. Rayner, N. A. et al. *J. Geophys. Res.* **108**, 4407 (2003).
17. Huang, B. et al. *J. Clim.* **34**, 2923–2939 (2021).
18. Donlon, C. J. et al. *Remote Sens. Environ.* **116**, 140–158 (2012).
19. Hersbach, H. et al. *Q. J. R. Meteorol. Soc.* **146**, 1999–2049 (2020).
20. Behringer, D. W. & Xue, Y. Evaluation of the global ocean data assimilation system at NCEP: the Pacific Ocean. Preprint at *Eighth Symp. on Integrated Observing and Assimilation Systems for Atmosphere, Oceans, and Land Surface* http://ams.confex.com/ams/84Annual/techprogram/paper_70720.htm (2004).

Acknowledgements

We appreciate the comments and suggestions from H. Wang, Y. Liu and D. Zhang. The scientific results and conclusions, as well as any views or opinions expressed herein, are ours and do not necessarily reflect the views of NWS, NOAA or the Department of Commerce. PMEL contribution no. 5638. This work was partially supported by Guangdong Major Project of Basic and Applied Basic Research (2020B0301030004; Y.L.) and the National Natural Science Foundation of China (42175056; Y.L.).

Author contributions

Z.-Z.H. and M.J.M. conceptualized the project, and Z.-Z.H. undertook the analysis, visualization, writing, reviewing and editing of the manuscript. The other authors (B.H., J.Z., and Y.L.) provided suggestions, and reviewed and edited the paper. All authors read and approved the final paper.

Competing interests

The authors declare no competing interests.

Additional information

Correspondence and requests for materials should be addressed to Zeng-Zhen Hu.

Peer review information *Nature Climate Change* thanks Jing-Jia Luo and the other, anonymous, reviewer(s) for their contribution to the peer review of this work.